mately 2mm (C_{2v}) point symmetry in which one of the mirror planes contains atoms in positions 12, 13, 18, and 19 of cage II and the other mirror plane is perpendicular to the first one and bisects the bonds between atoms 12–13 and 18–19. The twofold rotation axis is along the intersection of these two mirror planes. If the carbon atom in position 8 of cage I were disordered equally between positions 8 and 11, the anion would have 2mm point symmetry with respect to all atoms including borons and carbons. The axis of cage I, Co(1)–B(1), makes an angle of 117° with the axis of cage III, Co(2)–B(32); the ideal angle for regular icosahedra is 116.5°. The cages are arranged such that all of the carbon atoms lie on the interior side of this angle and are as close to each other as is possible in this staggered configuration.

The bond distances between all the atoms in the icosahedral framework except hydrogens are listed in Table V and the distances between the hydrogen atoms and the atoms to which they are bonded are given in Table VI. The standard deviations quoted on the bond distances in these tables are calculated from the least-squares estimates of the accuracy of the final positional parameters. Probably a better estimate of their accuracy is given by the larger root-mean-square deviations of equivalent bond distances from their average values, given in Table VII. A complete list of bond angles would be a rather long list indeed. Therefore, since both the cages I and III are analogous to the previously investigated 11-atom icosahedral fragments,[7] only the angles involving the 10-atom fragment, cage II, are reported in Table VIII.

The molecular packing in the crystal is shown in Figure 2 by a framework drawing of the projection of the unit cell contents along the *a* axis. This drawing, together with the distances given in Table IX, reveals a series of interactions among the cesium ions, the oxygens of the water molecules, and the hydrogen atoms attached to the anion. The cesium ions and the anion cages are held in their relative orientations by the balance of the attraction of their unlike charges with the repulsive forces of the electrons in the cesium ions and the hydrogen atoms attached to the cages. All of the shortest distances to the oxygen, given in Table IX, correspond to reasonable van der Waals contacts expected for a normal water of hydration.

TABLE IX

SHORTEST DISTANCES (Å) TO CESIUMS AND OXYGEN[a]

Atom	To O(1)	Atom	To Cs(1)	Atom	To Cs(2)
H(1)	2.76	H(18)	2.82	H(15)	2.95
H(24)	2.78	H(32)	2.95	H(4)	3.05
H(6)	2.78	H(17)	2.99	H(10)	3.08
H(17)	2.93	H(19)	3.00	H(24)	3.08
Cs(2)	3.029	H(11)	3.12	H(21)	3.10
Cs(1)	3.163	H(6)	3.15	H(6)	3.16
H(5)	3.21	H(29)	3.23	H(25)	3.25
H(21)	3.26	H(3)	3.24		
		H(30)	3.29		

[a] Estimated standard deviations are all ±0.05 Å except O(1) to Cs(1) and to Cs(2) which are ±0.006 Å.

Acknowledgment.—We wish to thank J. N. Francis and M. F. Hawthorne of the University of California, Riverside, Calif., for providing us with the crystals used in this work.

CONTRIBUTION FROM THE DEPARTMENT OF CHEMISTRY, CORNELL UNIVERSITY, ITHACA, NEW YORK 14850

The Structures of *gauche*- and *trans*-Tetrafluorohydrazine as Determined by Electron Diffraction

BY MARK J. CARDILLO AND S. H. BAUER

Received November 4, 1968

The interatomic distances, bond angles, and the proportions of *gauche* and *trans* isomers present in N_2F_4 have been determined by gas-phase electron diffraction. The two rotamers are similar in structure except for the dihedral angle ($\theta_g = 67.1 \pm 0.8°$). The 47% *gauche*–53% *trans* mixture found at below room temperature indicates that the *trans* is 300–500 cal more stable than the *gauche* rotamer. The bond lengths N–N = 1.489 ± 0.007 Å and N–F = 1.375 ± 0.004 Å are the same for both species but the valence angles are slightly different ($\angle FNF_g = 105.1 \pm 1.0°$, $\angle FNF_t = 102.9 \pm 0.75°$, $\angle F_1NN_g = 100.1 \pm 1.0°$, $\angle F_2NN_g = 104.3 \pm 1.0°$, $\angle FNN_t = 100.6 \pm 0.6°$). The nonbonded mean-square amplitudes show a strong angular dependence on the equilibrium geometry due to torsional motion about the N–N bond.

Introduction

The structure of tetrafluorohydrazine has been the subject of considerable discussion in recent years. The first experimental study was made with microwaves.[1] As is typical for fluorinated molecules only a limited amount of isotopically substituted species were available. For assumed bonded distances of N–N = 1.47 Å and N–F = 1.37 Å, the valence angles were found to be $\angle FNF = 108°$ and $\angle FNN = 104°$, with a dihedral angle of 65°; the estimated accuracy is 2–3°. The *trans* rotamer of N_2F_4 has C_{2h} symmetry and thus no dipole moment. The fact that the spectrum was observed indicated that a significant amount of the

(1) D. R. Lide and D. E. Mann, *J. Chem. Phys.*, **31**, 1129 (1959).

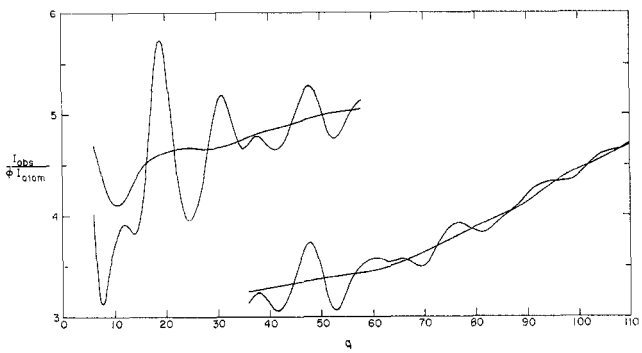

Figure 1.—Experimental intensity and final background curves for long and for short sample–plate distances after division by the product of I_{atomic} and the sector function (ϕ). The very slight, somewhat regular oscillations in the background curves for the short sample–plate distance data have approximately twice the period of that present in the long-distance data, as is expected from the slight regular fluctuations introduced in the determination of the sector function.

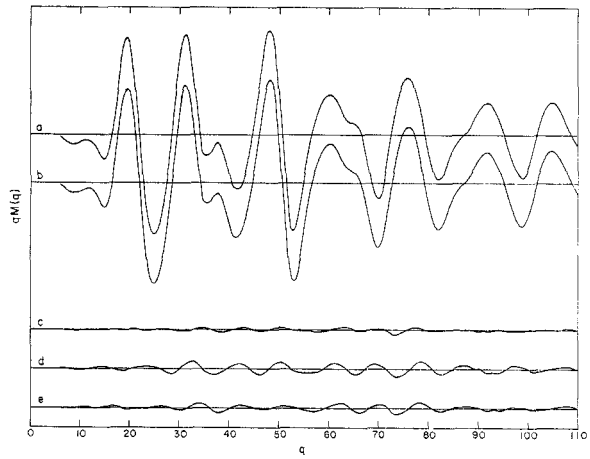

Figure 2.—(a) Experimental $qM(q)$; (b) theoretical $qM(q)$ for 47:53 *gauche–trans* model; (c) difference between (a) and (b); (d) corresponding difference curve for 60:40 *gauche–trans* model; (e) difference curve for 40:60 *gauche–trans* model.

gauche rotamer was present. A minimum rotational barrier of 3 kcal was implied.

Shortly thereafter both infrared[2] and Raman[3] spectra were recorded and analyzed. Each suggested independently that the presence of *gauche* rotamer alone was sufficient to account for the data. The infrared analysis included a fairly complete vibrational assignment. Electron diffraction photographs were then taken in this laboratory[4] using our old electron diffraction apparatus.[5] The gas was expanded into a seasoned glass vessel and the sample was maintained at room temperature. Although values of q [$= (40/\lambda)(\sin\theta/2)$] as low as 12 were observed, points below $q = 20$ were considered of questionable reliability; $q_{max} \approx 100$. The intensity curve appeared to be matched to acceptable precision by a model which consisted only of the *gauche* rotamer. The radial distribution function was consistent with this to the accuracy of its base line. However, a reexamination of this curve shows it to have fair-sized fluctuations.[4] The possibility of two rotamers with similar structures was not questioned inasmuch as the simplest model which satisfactorily accounted for the available data was consistent with previously reported studies.

These conclusions are currently disputed by reanalyses of the molecular vibrational spectra and by a low-temperature nmr study.[6] Over the range -145 to $-180°$ the nmr spectrum of N_2F_4 in several nonpolar solvents consists of five lines. These can be reasonably assigned by allocating one intense, sharp line to the *trans* species and the remaining four, which resemble an AB quartet, to the two *gauche* rotamers. Since the area ratio for singlet *vs.* quartet is 1.0 ± 0.1, the *trans* form appears to be lower in energy by about 200 cal/mol.

The recent Raman[7a] and infrared[7b] investigations substantiate this interpretation. From the number and mutual exclusion of fundamentals as assigned there is convincing evidence for the presence of two species with different symmetries. A considerable temperature variation showed no significant effect on the intensities and this supports the smallness of the energy difference between the rotamers. It is clear that the conclusion of the previous electron diffraction study with respect to the amount of *trans* present was not valid, and a reinvestigation was indicated. A detailed review of the previous structure determination[4] indicated two possible sources of error. With regard to the diffraction data, the first sample (in contrast with the procedure followed in the present experiment) was transferred several times in glass containers. Although precautions were taken to "season" these vessels there may have been some decomposition and the data as used may have had less than the best resolution. A second and more important point was raised regarding the data reduction procedure. Calculation of the radial distribution curve was limited to points in the range $q = 20$–100, and we started with a supposition that only one isomer was present. It appears that the test model inserted to supplement the experimental intensity curve for the range $0 < q < 20$ strongly influenced the area under the critical peak at 3.5 Å and thus strongly biased the deduction that the sample was predominantly the *gauche* isomer. Improvements available in the new apparatus[8] for recording the low-angle scattering region, substantial reduction of background scattering, plus significant advances in microphotometric techniques over those used in the first N_2F_4 study should provide the precision necessary to determine both the structures and ratio of the rotamers in N_2F_4.

(2) J. R. Durig and R. C. Lord, *Spectrochim. Acta*, **19**, 1877 (1963).
(3) Yu. I. Kutov and V. M. Tatevskii, *Opt. i. Spektroskopiya*, **14**, 443 (1963).
(4) R. K. Bohn and S. H. Bauer, *Inorg. Chem.*, **6**, 304 (1967).
(5) J. M. Hastings and S. H. Bauer, *J. Chem. Phys.*, **18**, 13 (1950).
(6) C. B. Colburn, F. A. Johnson, and C. Haney, *ibid.*, **43**, 4526 (1965).
(7) (a) J. R. Durig and J. W. Clark, *ibid.*, **48**, 3216 (1968); (b) D. F. Koster and F. A. Miller, *Spectrochim. Acta*, **24A**, 1487 (1968).
(8) S. H. Bauer and K. Kimura, *J. Phys. Soc. Japan, Suppl.*, **B-2**, 300 (1962).

TABLE I

EXPERIMENTAL INTENSITIES FOR N_2F_4

(Corrected for saturation; $q = (40/\lambda)\sin\theta/2$)

Long Distance

L = 254.0mm, λ = .04895Å

q	INTENSITY	qM(q)	q	INTENSITY	qM(q)
6.	0.8721	-128.6	45.	1.3543	+081.9
7.	0.8656	-273.3	46.	1.3948	258.7
8.	0.8112	-298.4	47.	1.4209	407.5
9.	0.8145	-231.3	48.	1.4297	456.7
10.	0.8418	-154.0	49.	1.4133	
11.	0.8703	-096.2	50.	1.3734	
12.	0.7001	-085.0	51.	1.3293	
13.	0.7261	-136.1	52.	1.3071	
14.	0.7465	-212.4	53.	1.3095	
15.	0.8024	-226.3	54.	1.3282	
16.	0.9109	-089.1	55.	1.3613	
17.	1.0717	+182.1	56.	1.3896	
18.	1.2401	490.6	57.	1.4097	
19.	1.3258	663.0	58.	1.4247	
20.	1.3217	588.0	59.	1.4358	
21.	1.2352	298.4	60.	1.4489	
22.	1.1364	-087.2	61.	1.4553	
23.	1.0616	-369.5	62.	1.4640	
24.	1.0324	-530.0	63.	1.4748	
25.	1.0457	-552.6	64.	1.4857	
26.	1.0892	-473.6	65.	1.4953	
27.	1.1538	-317.5			
28.	1.2386	-087.8		Short Distance	
29.	1.3243	+183.9		L = 126.2 λ = .0486	
30.	1.4039	407.6			
31.	1.4307	495.9	22.	3.2883	
32.	1.4150	402.9	23.	2.8599	
33.	1.3641	199.6	24.	2.7191	
34.	1.3113	= 0.0	25.	2.6798	
35.	1.2910	-100.2	26.	2.7106	
36.	1.2984	-093.4	27.	2.7884	
37.	1.3115	-050.1	28.	2.8663	
38.	1.3127	-047.1	29.	2.9715	
39.	1.3045	-106.7	30.	3.0232	
40.	1.2890	-191.2	31.	3.0052	
41.	1.2786	-247.1	32.	2.9047	
42.	1.2822	-245.7	33.	2.7895	
43.	1.2954	-184.1	34.	2.6573	
44.	1.3179	-070.5	35.	2.6007	

q	INTENSITY	qM(q)	q	INTENSITY	qM(q)	q	INTENSITY	qM(q)
36.	2.5845		75.	2.7459	210.9	114.	3.2483	
37.	2.5878		76.	2.7586	222.6	115.	3.2766	
38.	2.5660		77.	2.7607	191.9	116.	3.3067	
39.	2.5284		78.	2.7581	125.2	117.	3.3290	
40.	2.4933		79.	2.7484	037.5	118.	3.3611	
41.	2.4618		80.	2.7389	-062.4	119.	3.3867	
42.	2.4519		81.	2.7336	-136.1	120.	3.4100	
43.	2.4831		82.	2.7362	-169.0	121.	3.4318	
44.	2.5231		83.	2.7563	-132.1			
45.	2.5735		84.	2.7759	-105.9			
46.	2.6347		85.	2.7947	-057.5			
47.	2.6812		86.	2.8105	-025.3			
48.	2.6888	456.7	87.	2.8267	-004.9			
49.	2.6493	353.9	88.	2.8461	+015.9			
50.	2.5753	118.3	89.	2.8653	52.8			
51.	2.4914	-158.5	90.	2.8826	85.5			
52.	2.4457	-358.8	91.	2.9000	114.1			
53.	2.4292	-413.5	92.	2.9102	118.5			
54.	2.4661	-333.3	93.	2.9210	95.6			
55.	2.5180	-188.4	94.	2.9314	66.8			
56.	2.5527	-052.1	95.	2.9372	24.0			
57.	2.5827	+047.7	96.	2.9430	- 35.3			
58.	2.5997	110.5	97.	2.9488	- 94.9			
59.	2.6158	149.9	98.	2.9533	-137.2			
60.	2.6314	166.8	99.	2.9719	=156.1			
61.	2.6400	154.8	100.	2.9972	=125.1			
62.	2.6447	118.8	101.	3.0266	- 62.8			
63.	2.6464	073.7	102.	3.0570	+ 11.3			
64.	2.6499	052.7	103.	3.0815	74.2			
65.	2.6495	047.6	104.	3.0999	110.2			
66.	2.6455	028.3	105.	3.1142	117.1			
67.	2.6313	-033.0	106.	3.1260	100.6			
68.	2.6138	-129.9	107.	3.1322	69.9			
69.	2.6010	=221.2	108.	3.1477	31.6			
70.	2.6031	-253.7	109.	3.1594	= 6.2			
71.	2.6236	-204.0	110.	3.1703	- 36.1			
72.	2.6631	-084.1	111.	3.1847				
73.	2.6994	+056.5	112.	3.2009				
74.	2.7233	157.3	113.	3.2253				

EXPERIMENTAL REDUCED INTENSITIES FOR N_2F_4

(corrected for plate saturation and flatness; devided by arbitrarily normalized sector function (Φ) and calculated atomic intensity; $q = 40/\lambda \sin\theta/2$)

Long Distance

L = 254.0 mm; λ = .04895Å

q	$I_{obs}/\Phi I_{atom}$	q	$I_{obs}/\Phi I_{atom}$	q	$I_{obs}/\Phi I_{atom}$	q	$I_{obs}/\Phi I_{atom}$
4.	7.163	49.	5.364	41.	1.3139	86.	1.5017
5.	5.798	50.	5.203	42.	1.3132	87.	1.5092
6.	4.086	51.	5.055	43.	1.3251	88.	1.5179
7.	3.391	52.	4.947	44.	1.3484	89.	1.5303
8.	3.349	53.	4.935	45.	1.3782	90.	1.5405
9.	3.581	54.	5.003	46.	1.4102	91.	1.5519
10.	3.841	55.	5.106	47.	1.4374	92.	1.5591
11.	3.996	56.	5.194	48.	1.4471	93.	1.5633
12.	4.070	57.	5.264	49.	1.4318	94.	1.5662
13.	4.040	58.	5.312	50.	1.3954	95.	1.5672
14.	3.987	59.	5.357	51.	1.3503	96.	1.5674
15.	4.126	60.	5.401	52.	1.3199	97.	1.5691
16.	4.508	61.	5.417	53.	1.3136	98.	1.5694
17.	5.071	62.	5.414	54.	1.3292	99.	1.5720
18.	5.609	63.	5.418	55.	1.3541	100.	1.5799
19.	5.854	64.	5.425	56.	1.3762	101.	1.5901
20.	5.660	65.	5.441	57.	1.3941	102.	1.5997
21.	5.187	66.	5.462	58.	1.4054	103.	1.6110
22.	4.667	67.	5.422	59.	1.4097	104.	1.6176
23.	4.279	68.		60.	1.4165	105.	1.6219
24.	4.095			61.	1.4158	106.	1.6265
25.	4.105		Short Distance	62	1.4118	107.	1.6298
26.	4.226		L = 126.2 mm,	63.	1.4091	108.	1.6309
27.	4.419		λ = .0486 Å	64.	1.4114	109.	1.6352
28.	4.695			65.	1.4122	110.	1.6399
29.	4.997			66.	1.4141	111.	1.6452
30.	5.224	22.	1.2052	67.	1.4105	112.	1.6536
31.	5.294	23.	1.1268	68.	1.4045	113.	1.6615
32.	5.204	24.	1.1105	69.	1.3997	114.	1.6727
33.	5.030	25.	1.1217	70.	1.4014	115.	1.6820
34.	4.873	26.	1.1572	71.	1.4106	116.	1.6899
35.	4.817	27.	1.2130	72.	1.4303	117.	1.6972
36.	4.855	28.	1.2664	73.	1.4590	118.	1.7060
37.	4.909	29.	1.3606	74.	1.4699	119.	1.7136
38.	4.926	30.	1.4155	75.	1.4770	120.	1.7211
39.	4.883	31.	1.4238	76.	1.4840	121.	1.7285
40.	4.834	32.	1.4046	77.	1.4846		
41.	4.813	33.	1.3697	78.	1.4804		
42.	4.826	34.	1.3248	79.	1.4786		
43.	4.891	35.	1.3269	80.	1.4698		
44.	4.997	36.	1.3268	81.	1.4688		
45.	5.137	37.	1.3430	82.	1.4678		
46.	5.281	38.	1.3481	83.	1.4749		
47.	5.397	39.	1.3406	84.	1.4838		
48.	5.431	40.	1.3272	85.	1.4934		

Experimental Section

A sample of N_2F_4 in a Monel cylinder was received from Dr. Charles Colburn. The purity was reported to be better than 97%, with the principal impurities being N_2F_2 (0.66%), NO (0.93%), N_2 (0.59%), N_2O (0.41%), and NF_3 (0.26%). The cylinder was attached directly by a short stainless steel tube to the nozzle inlet system of the new electron diffraction apparatus. The cylinder was then cooled to about −140°, and all surfaces (valve, lead tubes, nozzle) were seasoned by lengthy bleeding of sample prior to recording the photographs. This bleeding out of sample helped to cool the inner tubing slightly. No quantitative estimate of the gas temperature as emitted from the nozzle could be made.

Light and dark sectored photographs were taken at 65 kV for two sample–plate distances: 12 and 26 cm. The observed scattering extended over $6 < q < 128$. An MgO pattern was recorded for each set of conditions to provide wavelength calibration. The diffraction patterns were scanned along a diameter on a Jarrell-Ash microdensitometer, fitted with a rapidly rotating stage. The output was fed to a digital converter and recorded to five figures. The plate drive was monitored by a shaft encoder which has a precision of 1 μ per reading. A scale vernier, which permits checking on the total distance to a few microns, was

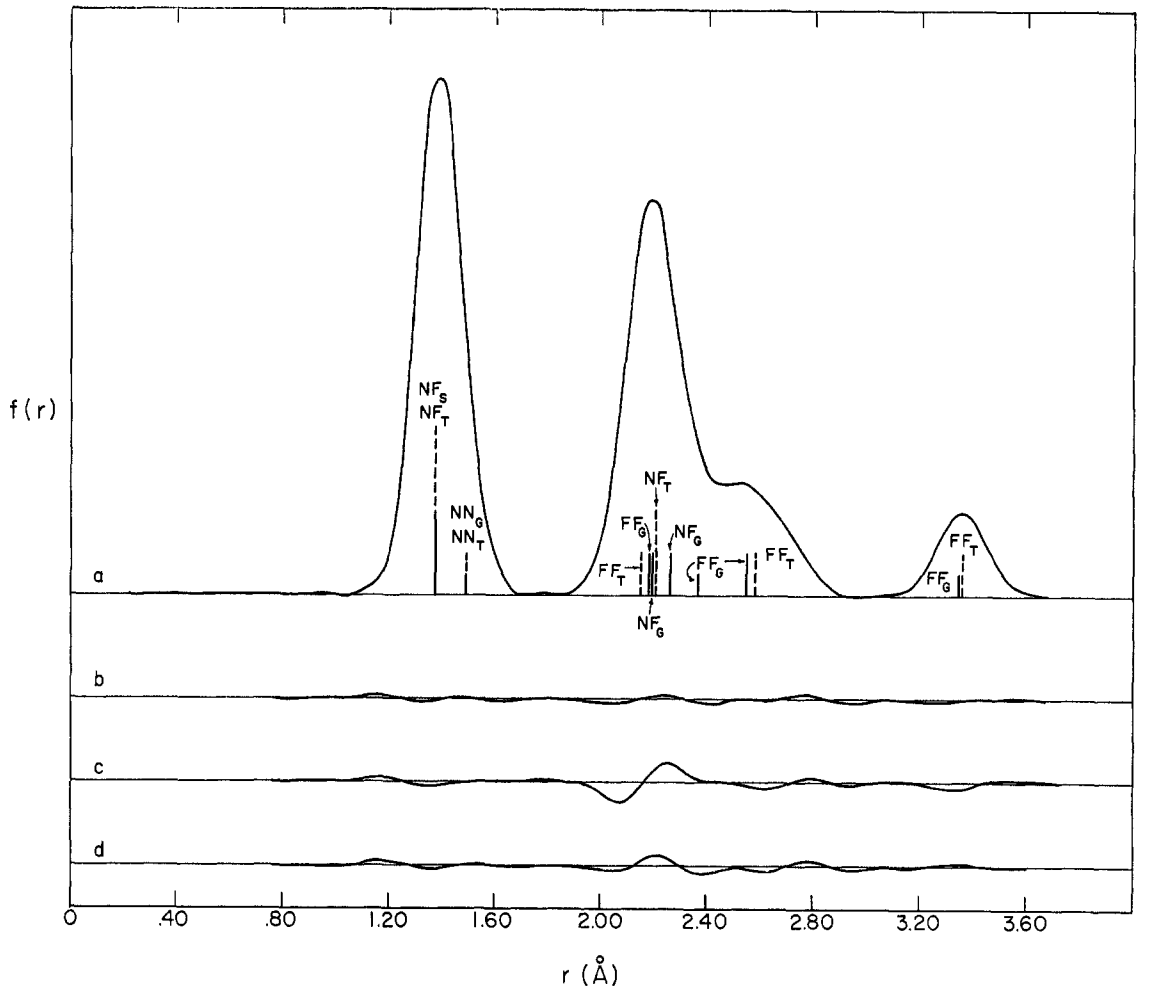

Figure 3.—(a) Experimental radial distribution function f(*r*); (b) difference curve between the experimental and that for 47:53 *gauche–trans* model; (c) difference curve for 60:40 *gauche–trans* model; (d) difference curve for 40:60 *gauche–trans* model.

mounted directly onto the traveling stage. Optical densities were converted to intensities in a manner previously described.[9]

Reduction of Data

The sector used was cut to fit the reciprocal of the carbon atom scattering intensity. It was then calibrated by comparison of scattering produced by Ar with that calculated from the tabulated atom form factor. Except for the inner quarter, the calculated and the measured aperture functions agreed to within 2%.

The experimentally measured sector function $\phi(r)$ was tabulated and divided into the N_2F_4 total intensity values, along with the atomic intensity. The latter was calculated using Bonham's[10] form factors for elastic scattering and Tavard's[11] inelastic scattering factors. This procedure permits one simply to subtract the background. In principle, the observed intensity is a superposition of the terms

$$I_{obsd} = k\{\phi[I_{mol} + I_{atomic} + I_{back}] + I'_{back}\}$$

where I_{back} and I'_{back} represent sectored and unsectored backgrounds, and ϕ is the sector function. On dividing I_{obsd} by the product of the sector function and I_{atomic}

$$\frac{I_{obsd}}{\phi I_{atomic}} \propto \left[\frac{I_{mol}}{I_{atomic}} + \left\{1 + \frac{I_{back}}{I_{atomic}} + \frac{I'_{back}}{\phi I_{atomic}}\right\}\right]$$

we obtained Figure 1, in which the quantity on the right was drawn to an arbitrary scale. This scale depends on the normalization of the tabulated sector function. The background line, drawn in after refinement of the radial distribution curve, is subtracted from the original curve. The difference is proportional to $M(q)$ or I_{mol}/I_{atomic}. This procedure removes most but not all of the variable resolution factor generally observed in conventional analyses. The procedure for refinement of this background is now conventional, *i.e.*, the elimination of negative areas and fluctuations in the nonstructural regions of the radial distribution curve.[12] The inaccuracy of the sector *function* determination at low scattering angles is primarily responsible for the shape of the background curve at low q values. However, this background shape is the same as that obtained for many other

(9) (a) J. L. Hencher and S. H. Bauer, *J. Am. Chem. Soc.*, **89**, 5527 (1967); (b) W. Harshbarger, G. Lee, R. F. Porter, and S. H. Bauer, *Inorg. Chem.*, **8**, 1683 (1969).

(10) H. L. Cox, Jr., and R. A. Bonham, *J. Chem. Phys.*, **47**, 2599 (1967).

(11) C. Tavard, D. Nicolas, and M. Rouault, *J. Chim. Phys.*, **64**, 540 (1967).

(12) (a) J. Karle and I. L. Karle, *J. Chem. Phys.*, **18**, 957 (1950); L. S. Bartell, L. O. Brockway, and R. H. Schwendeman, *ibid.*, **23**, 1854 (1955).

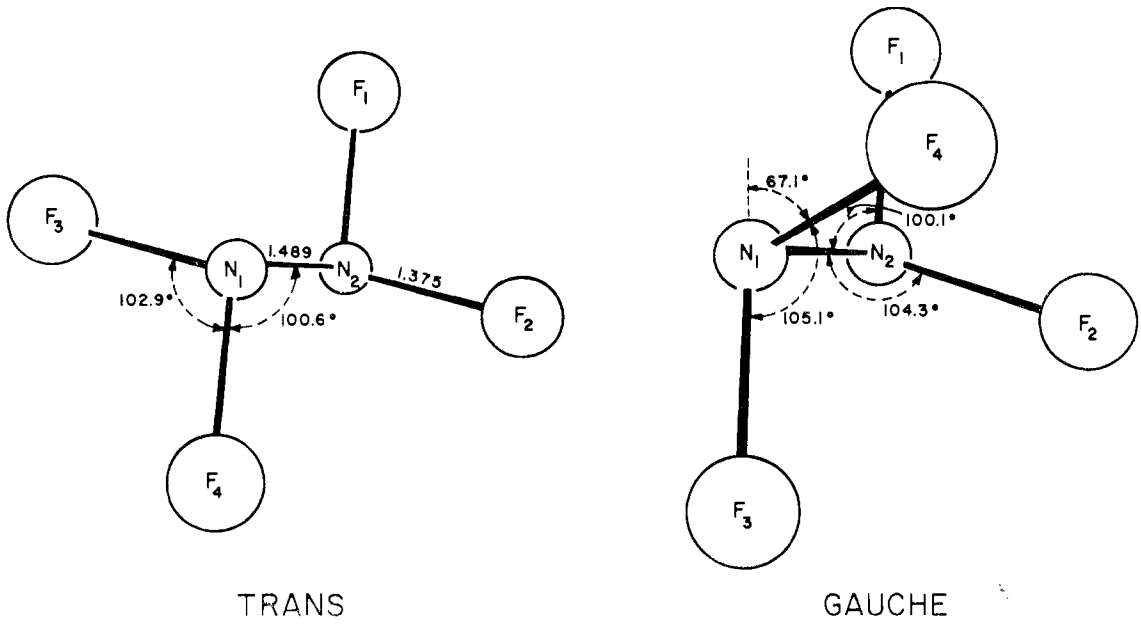

Figure 4.—Representation of the two rotamers of N_2F_4.

molecules for which the same sector was used and supports the reliability of the $qM(q)$ function at low q values. The $qM(q)$ function (Table I, Figure 2) was corrected for electronic scattering on the basis of the model being tested to permit a radial distribution refinement. A damping factor of $\gamma = 0.0019$ was included in the Fourier inversion of the nuclear intensity.

Analysis and Results

A preliminary set of parameters was obtained from the refined radial distribution function (Figure 3). Particular attention was devoted to the isolated nonbonded peak at 3.36 Å. The area is determined by the *gauche*:*trans* ratio and can vary up to 50% on going from no *gauche* to all *gauche* because this rotamer has one F–F distance at this separation whereas the *trans* has two. The smoothness of the base line for the final experimental f(r) curve indicates the area of the 3.36-Å nonbonded peak may be utilized as a reliable parameter, provided the low-angle diffraction data are properly corrected for nonnuclear scattering. It soon became evident that the two rotamers were present in approximately equal proportions.

After the bonded parameters, the mean-square amplitudes and the isomer ratio were estimated by fitting the f(r) curve, an extensive least-squares analysis was undertaken to deduce the final parameters. The convergence of the least-squares programs was seriously hampered by the fact that the two rotamers were independent yet so structurally similar. It was necessary to constrain the concentration ratio to a sequence of values and for each ratio to allow the remaining parameters to vary. The criterion of lowest standard deviation in fitting the intensity curve was used to select the final parameters listed in Table II. Figure 4 is an illustration of the two rotamers.

TABLE II
GEOMETRIC PARAMETERS FOR N_2F_4[a]

	gauche	*trans*
N–N, Å	1.489 ± 0.004	1.489 ± 0.004
N–F, Å	1.375 ± 0.004	1.375 ± 0.004
∠F_1NF_2, deg	105.1 ± 1.5	102.9 ± 1.0
∠F_1NN, deg	100.1 ± 1.5	100.6 ± 0.6
∠F_2NN, deg	104.3 ± 1.0	100.6 ± 0.6
θ(dihedral), deg	67.1 ± 1.0	180.0
l(N–N), Å	0.044 ± 0.004	0.044 ± 0.004
l(N–F), Å	0.045 ± 0.003	0.045 ± 0.003
l(N_1–F_2), Å	0.094 ± 0.006	0.094 ± 0.006
l(F_1–F_2), Å	0.053 ± 0.004	0.053 ± 0.004
l(F_1–F_3), Å	0.068 ± 0.012	0.113 ± 0.030
l(F_1–F_4), Å	0.120 ± 0.030	0.070 ± 0.007
l(F_2–F_4), Å	0.118 ± 0.026	0.113 ± 0.030

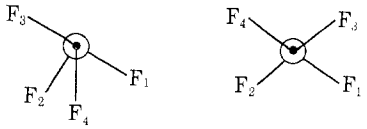

[a] Basis: *gauche*:*trans* = 47:53. See text for comments on error estimates.

Throughout the least-squares analysis only those *gauche*:*trans* ratios between 40:60 and 50:50 converged either to a minimum or to a small oscillating sequence of residuals whereas ratios beyond these limits diverged. The standard deviation appears to have two minima, the lowest at 47:53 and another, significantly higher, at 43:57 for a slightly different set of geometric parameters. When the ratio was fixed at 40:60, the deduced mean-square amplitudes became unacceptable.

The differences between the 47:53 *gauche*:*trans* model and the experimental $qM(q)$ and f(r) curves are shown in Figures 2 and 3. Also included are the difference curves for 40:60 and 60:40 ratios. One may estimate from both drawings that the 47:53 ratio best represents the diffraction data to about 3%, from the

TABLE III

ERROR MATRIX FOR N_2F_4 (MIXTURE)[a]

	N–N	N–F	∠FNF$_g$	∠F$_2$NN$_g$	∠F$_2$NN$_g$	θ_g	∠FNF$_t$	∠FNN$_t$
N–N	+0.0021							
N–F	+0.0008	+0.0007						
∠FNF$_g$	+0.0160	−0.0049	+0.4465					
∠F$_1$NN$_g$	−0.0198	−0.0099	+0.0851	+0.2407				
∠F$_2$NN$_g$	−0.0014	−0.0034	−0.1786	+0.0602	+0.1032			
θ_g	+0.0119	+0.0037	+0.1790	−0.1029	−0.0884	+0.1348		
∠FNF$_t$	−0.0116	−0.0039	−0.2837	+0.0218	+0.1258	−0.1204	+0.2077	
∠FNN$_t$	−0.0083	−0.0019	−0.2294	−0.0645	+0.0968	−0.1077	+0.1519	+0.1425

[a] Distances in ångströms; angles are in degrees. The diagonal elements are the standard deviations for the corresponding parameters; the off-diagonal elements measure the correlation between the pairs involved. In this least-squares calculation the mean-square amplitudes and the *gauche*:*trans* ratio were held fixed. Prior to this, the geometric parameters were constrained and the amplitudes were allowed to vary. Deviations were determined by

$$\sigma_{ij} = \mathrm{sgn}[(BJ^{-1})_{ij}][|([B]^{-1})_{ij}|\chi_R/(n_q - n_p)]^{1/2}; \quad [B] \equiv [J]^t[w][J]$$

where χ_R is the sum of the squares of the residuals, n_q is the number of observations (105, at integral q's), n_p is the number of varied parameters (8), $[J]$ is the Jacobian matrix, $[w]$ is the weight matrix, $w = \exp[-w_1(q_1 - q)]$ for $q < q_1 = 20$, $w = 1$ for $q_1 < q < q_2$, $w = \exp[-w_2(q - q_2)]$ for $q < q_2 = 105$, and w_1 and w_2 are adjusted so that $w(q_{max}) = 0.85$ and $w(q_{min}) = 0.35$.

magnitude of the discrepancies with respect to the larger departures. It is also apparent that the radial distribution function is a good means for determining the percentages of *gauche* and *trans*. The significant structural difference between the rotamers is one nonbonded fluorine–fluorine distance, which is near 2.3 Å for the *gauche* but 3.5 Å in the *trans*. This amounts to a change in periods from 20/2.3 to 20/3.5 for one of the many sinusoidal contributions which comprise the intensity curve. For a sequence of models with slightly different ratios this small difference, spread over the entire diffraction curve, is often the same magnitude as the "random" error, as illustrated in curves d and e of Figure 2. However in the radial distribution curve these differences accumulate into two areas, readily visible. Curves c and d of Figure 3 clearly demonstrate this.

The errors quoted in Table II were estimated as follows. One of the larger sources of error for the bonded distances is the systematic calibration error due to the possible misalignment of the MgO sample with the nozzle. The standard deviation in the least-squares fit (Table III) of the N–F distance is less than 0.001 Å, but the uncertainty in placing the MgO sample above the inlet nozzle allows a scale error of almost 0.2% in the scale factor calibration. Thus ±0.004 Å represents safe limits for the error in the N–F bond distance. The standard deviation for the N–N distance is 0.002 Å; the error limits ±0.007 Å thus incorporate a range of more than three times the standard deviation.

The error limits for the angles are not as simply determined. They were generally fitted to about 0.5° by least-squares analyses for any fixed *gauche*:*trans* ratio. The scale factor error amounts to less than 1° as calculated from the bonded and nonbonded distances, if considered as independently determined. However, for different ratios within the 3% range of 47:53, these angles converged to values as much as 2° apart. To the extent that the ratio is uncertain, the angles as a correlated set have an uncertainty of up to 2°. However, this does not negate the reality of the converged differences between the angles, as reported, since these differences appear consistently for all assumed *gauche*:*trans* ratios. The errors reported encompass both of these considerations.

Discussion

This electron diffraction investigation confirms the findings of nmr[6] and molecular spectroscopists[7] that nearly equal amounts of *gauche* and *trans* rotamers are present in equilibrium samples of N_2F_4. The 47% *gauche*–53% *trans* (±3%) proportion found here is of considerably greater reliability than the previous electron diffraction study because of the dependence of the estimated ratio on the low-angle diffraction data, which are now available. From this ratio one can make but a rough estimate of the difference in energies of the two species, since no reliable value for the gas temperature at the point of diffraction is known. The gas was warmed considerably after leaving the −140° bath and possibly reached room temperature, as it flowed through the valve and tubing. However, it then cooled upon expansion on exit through the nozzle into the vacuum chamber. The sample at the point of diffraction is between 150 and 250°K. On this basis, it appears that the *trans* is 300–500 cal more stable than either *gauche* rotamer. This estimate agrees well with the 100–200 cal based on the nmr spectra.

The valence angles of both *gauche*- and *trans*-N_2F_4 are similar to those reported previously.[4] The differences in the corresponding parameters are real, since these were derived from the least-squares reductions for all ratios tested. The bonded distances N–F = 1.375 (4) Å and N–N = 1.489 (7) Å are somewhat shorter than those reported previously and are of higher precision. In Table IV these results are compared with the geometries of related molecules. It is interesting to note that the phosphorus compounds exhibit a trend similar to those of nitrogen. P_2H_4 is all *gauche*, whereas P_2F_4, P_2Cl_4, and P_2I_4 appear to be all *trans*; N_2H_4 is all *gauche*, but N_2F_4 is half *gauche* and half *trans*. The

TABLE IV
STRUCTURAL PARAMETERS FOR RELATED MOLECULES

Molecule	N–N, Å	∠NNX, deg	N–X, Å	*gauche*:*trans*	Ref
NF_2			1.363 ± 0.008		*a*
NF_3			1.371		*b*
N_2F_4	1.489 ± 0.004	100–104	1.375 ± 0.004	47:53	
N_2H_4	1.453 ± 0.003	112–112.5	1.022 ± 0.003	100:0	*c*
$N_2(CF_3)_4$	1.40 ± 0.02	119 ± 1.5	1.43 ± 0.01	100:0	
				(nearly planar)	*d*
$H_2N_2(CH_3)_2$	1.45 ± 0.03	110 ± 4	1.47 ± 0.03		*e*
N_2O_4	1.75	113.1	1.18	Planar	*f*
P_2H_4				100:0	*g*
P_2F_4				0:100	*h*
P_2Cl_4				0:100	*i*
P_2I_4	2.21 ± 0.06	94	2.48 ± 0.03	0:100	*j*

[a] Reference 4. [b] J. Sheridan and W. Gordy, *Phys. Rev.*, **79**, 513 (1950). [c] A. Yamaguchi, *et al.*, *J. Chem. Phys.*, **31**, 843 (1959). [d] L. S. Bartell and H. K. Higgenbotham, *Inorg. Chem.*, **4**, 1346 (1965). [e] W. Beamer, *J. Am. Chem. Soc.*, **70**, 2979 (1948). [f] D. W. Smith and K. Hedberg, *J. Chem. Phys.*, **25**, 1282 (1956). [g] E. R. Nixon, *J. Phys. Chem.*, **60**, 1054 (1956); M. Baudler and L. Schmidt, *Naturwissenschaften*, **44**, 488 (1957). [h] R. W. Rudolph, W. C. Taylor, and R. W. Parry, *J. Am. Chem. Soc.*, **88**, 3729 (1966). [i] S. G. Frankiss and F. A. Miller, *Spectrochim. Acta*, **21**, 1235 (1965). [j] S. G. Frankiss, F. A. Miller, H. Stammreich, and Th. Teixeira Sans, *ibid.*, **23A**, 543 (1967); Y. C. Leung and J. Waser, *J. Phys. Chem.*, **60**, 539 (1956).

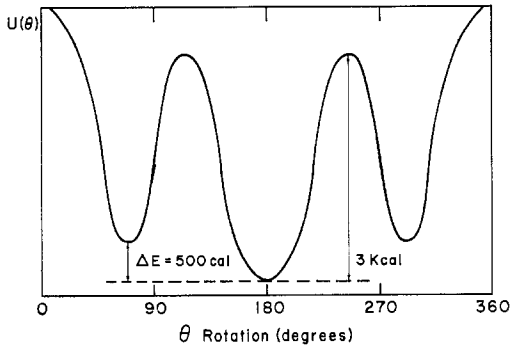

Figure 5.—Schematic drawing of rotational potential function assuming $E_{trans} - E_{gauche} = 500$ cal and the rotational barrier is +3 kcal.

species N_2O_4 and $N_2(CF_3)_4$ do not fit into this sequence, since the former is planar and the latter nearly so, and both show significant "distortions" in other molecular parameters as well.

The N–F bond length in N_2F_4 is very close to the value reported for NF_2 and NF_3. In contrast, the N–N single bond length is significantly different from those in N_2H_4 and $N_2(CF_3)_4$. It appears that the length of this bond correlates well with over-all molecular stability. The N–N bond dissociation energy in N_2H_4 is 60 kcal as compared to 20 kcal/mol in N_2F_4; the corresponding distances are 1.45 and 1.49 Å, respectively. $N_2(CF_3)_4$ is described as being extremely stable to decomposition and has the smallest bond length (1.40 Å).

The nonbonded mean-square amplitudes correlate with the magnitude of the dihedral angle, as discussed by Karle.[13] Possibly, a more extensive electron diffraction study, in which great care is taken to record accurately the low-angle scattering and to eliminate extraneous background scattering, may lead to a separation of the torsional motion from frame vibration and permit a closer estimate of the rotational barrier heights. These are presently estimated between 3 and 7 kcal.[1,6] One could then plot the total rotational potential function for motion around N–N. The general shape is schematically shown in Figure 5, using the presently estimated parameters. The minima at 67 and 293° are the *gauche* equilibrium positions. The increased stability of the *trans* species is indicated.

Acknowledgments.—The authors sincerely thank Dr. Charles Colburn for the generous sample of N_2F_4. This work was supported by the Material Science Center (MSC ARPA SD-68).

(13) J. Karle, *J. Chem. Phys.*, **45**, 4149 (1966).